

The Journal of Infectious Diseases

Probing of a human proteome microarray with a recombinant pathogen protein reveals a novel mechanism by which hookworms suppress B cell receptor signaling --Manuscript Draft--

Manuscript Number:	55213R1
Full Title:	Probing of a human proteome microarray with a recombinant pathogen protein reveals a novel mechanism by which hookworms suppress B cell receptor signaling
Short Title:	Host-pathogen interactions using protein microarrays
Article Type:	Major Article
Section/Category:	Parasites
Keywords:	Hookworm, Necator americanus, Na-ASP-2, SCP/TAPS, CD79, B cell, antigen receptor, protein microarray, host-pathogen interaction
Corresponding Author:	Alex Loukas James Cook University Cairns, QLD AUSTRALIA
Corresponding Author Secondary Information:	
Corresponding Author's Institution:	James Cook University
Corresponding Author's Secondary Institution:	
First Author:	Leon Tribolet
First Author Secondary Information:	
Order of Authors:	Leon Tribolet Cinzia Cantacessi Darren Pickering Severine Navarro Denise Doolan Angela Trieu Huang Fei Yang Chao Andreas Hofmann Robin Gasser Paul Giacomini Alex Loukas
Order of Authors Secondary Information:	
Manuscript Region of Origin:	AUSTRALIA
Abstract:	Na-ASP-2 is an efficacious hookworm vaccine antigen; however, despite elucidation of its crystal structure and studies addressing its immunobiology, the function of Na-ASP-2 has remained elusive. We probed a 9,000 protein human proteome microarray with Na-ASP-2 and showed binding to CD79A, a component of the B cell antigen receptor complex. Na-ASP-2 bound to human B lymphocytes ex vivo and down-regulated the transcription of ~1,000 B cell mRNAs, while only ~100 mRNAs were up-regulated compared to control-treated cells. The expression of a range of molecules was affected by Na-ASP-2, including factors involved in leukocyte transendothelial migration pathways and the B cell signaling receptor pathway. Of note was the down-regulated

transcription of lyn and pi3k, molecules that are known to interact with CD79A and control B cell receptor signaling processes. Together, these results highlight a previously unknown interaction between a hookworm-secreted protein and B cells, which has implications for helminth-driven immunomodulation and vaccine development. Further, the novel use of human protein microarrays to identify host-pathogen interactions, coupled to ex vivo binding studies and subsequent analyses of global gene expression in human host cells, demonstrates a new pipeline by which to explore the molecular basis of infectious diseases.

1 **Probing of a human proteome microarray with a recombinant pathogen protein reveals a**
2 **novel mechanism by which hookworms suppress B cell receptor signaling**

3

4 Leon Tribolet¹, Cinzia Cantacessi^{1,2}, Darren A. Pickering¹, Severine Navarro¹, Denise L. Doolan³,
5 Angela Trieu³, Huang Fei⁴, Yang Chao⁴, Andreas Hofmann⁵, Robin B. Gasser⁶, Paul R. Giacomin^{1*}
6 and Alex Loukas^{1*}

7

8 ¹Centre for Biodiscovery and Molecular Development of Therapeutics, Australian Institute of
9 Tropical Health and Medicine, James Cook University, Cairns, QLD 4878, Australia

10 ²Department of Veterinary Medicine, University of Cambridge, Cambridge CB30ES, United
11 Kingdom

12 ³QIMR Berghofer Medical Research Institute, Brisbane, QLD 4006, Australia

13 ⁴BGI-Shenzhen, Shenzhen 518083, China

14 ⁵Eskitis Institute, Griffith University, Brisbane, QLD 4111, Australia

15 ⁶Faculty of Veterinary Science, The University of Melbourne, Melbourne, VIC 3010, Australia

16

17

18 *Equal contributions.

19

20 Abstract word count: 195

21 Body Text word count: 3500

22

23

24 ***Running head.*** Hookworm protein regulates B cell receptor signaling

25

26

27 **FOOTNOTE PAGE**

28 ***Conflict of Interest.***

29 All authors have submitted the ICMJE Form for Disclosure of Potential Conflicts of Interest. The
30 authors do not have a commercial or other association that might pose a conflict of interest.

31

32 ***Funding.***

33 This work was supported by the Australian Research Council [Linkage Project grant 100100092 to
34 R.B.G, A.H., A.L.]; National Health and Medical Research Council (NHMRC) [Program Grant
35 1037304 to A.L. and D.L.D.; NHMRC Overseas Biomedical Fellowship 613718 to P.G.; NHMRC
36 Early Career Research Fellowship 1052936 to C.C.; NHMRC Principal Research Fellowships
37 1020114 to A.L. and 1023636 to D.L.D.]; Victoria Life Sciences Computation Initiative [VLSCI
38 VR0007 to R.B.G.] on its Peak Computing Facility at the University of Melbourne - an initiative of
39 the Victorian Government, and an Australian Postgraduate Award from James Cook University
40 [L.T].

41

42 ***Corresponding author.***

43 Alex Loukas, Australian Institute of Tropical Health and Medicine, QTHA Building E4, James
44 Cook University, McGregor Road, Smithfield, QLD, Australia, 4878. ph: +61 7 4232 1608,
45 alex.loukas@jcu.edu.au

46

47 **ABSTRACT**

48

49 ***Na*-ASP-2 is an efficacious hookworm vaccine antigen; however, despite elucidation of its**
50 **crystal structure and studies addressing its immunobiology, the function of *Na*-ASP-2 has**
51 **remained elusive. We probed a 9,000 protein human proteome microarray with *Na*-ASP-2**
52 **and showed binding to CD79A, a component of the B cell antigen receptor complex. *Na*-ASP-**
53 **2 bound to human B lymphocytes ex vivo and down-regulated the transcription of ~1,000 B**
54 **cell mRNAs, while only ~100 mRNAs were up-regulated compared to control-treated cells.**
55 **The expression of a range of molecules was affected by *Na*-ASP-2, including factors involved**
56 **in leukocyte transendothelial migration pathways and the B cell signaling receptor pathway.**
57 **Of note was the down-regulated transcription of *lyn* and *pi3k*, molecules that are known to**
58 **interact with CD79A and control B cell receptor signaling processes. Together, these results**
59 **highlight a previously unknown interaction between a hookworm-secreted protein and B cells,**
60 **which has implications for helminth-driven immunomodulation and vaccine development.**
61 **Further, the novel use of human protein microarrays to identify host-pathogen interactions,**
62 **coupled to ex vivo binding studies and subsequent analyses of global gene expression in**
63 **human host cells, demonstrates a new pipeline by which to explore the molecular basis of**
64 **infectious diseases.**

65

66 ***Keywords.*** Hookworm, *Necator americanus*, *Na*-ASP-2, SCP/TAPS, CD79, B cell, antigen
67 receptor, protein microarray, host-pathogen interaction

68 **INTRODUCTION**

69 The hookworm *Necator americanus* is one of the most prevalent pathogens of humans, infecting
70 between 576-740 million people worldwide [1]. Hookworms can persist for many years within their
71 hosts [2], having evolved a suite of strategies to evade immune attack, from the point of per-
72 cutaneous entry and pulmonary migration by third-stage larvae (L3), through to their final site of
73 residence as adult worms in the gut. While hookworm infection can be treated with anthelmintic
74 drugs, reinfection rapidly occurs [3], precipitating an urgent need for development of vaccines to
75 limit the global burden of human hookworm infections [4].

76
77 Efforts to develop vaccines against hookworm infection have focused on discovery of antigens
78 secreted by the L3 stage. Serum antibodies from dogs vaccinated with irradiated hookworm L3 [5]
79 and people from hookworm-endemic areas with high antibody titres but low egg counts [6]
80 predominantly recognise members of the activation-associated protein (ASP) family, notably *Na*-
81 ASP-2. In a phase 1a vaccine trial in hookworm naïve subjects from the U.S., recombinant *Na*-
82 ASP-2 was well-tolerated and immunogenic [7], however, a phase 1b trial in hookworm-exposed
83 individuals in Brazil was halted due the development of urticarial reactions in people with pre-
84 existing IgE against *Na*-ASP-2 [8]. Despite the safety concerns, there remains interest in *Na*-ASP-2
85 as a vaccine candidate, particularly if used as a pediatric vaccine prior to the development of anti-
86 hookworm IgE responses, or if it is modified to reduce its allergenic capacity [9]; which has proven
87 effective for peanut, dust mite and wasp allergens [10-12].

88
89 Despite the relatively long history of research into hookworm ASPs as vaccines, relatively little is
90 known about their biological roles. ASP-2 is one of the most abundant excretory/secretory (ES)
91 proteins produced by L3 upon exposure to host serum [13, 14], however its expression is
92 diminished as the parasite migrates through the lung, provoking the hypothesis that ASP-2 may be
93 involved in immune regulation while the parasite resides in the circulatory system. Administration

94 of recombinant *Na*-ASP-2 to rodents elicits a type 2 cytokine response, robust antibody production
95 and neutrophil recruitment [5, 15], although direct interactions between *Na*-ASP-2 and a defined
96 cell type were not elucidated. The hookworm ASP protein family forms 3 distinct structural groups
97 based on X-ray crystallographic studies [16, 17]. The crystal structure of *Na*-ASP-2 indicates the
98 presence of a putative electronegative binding cavity flanked by conserved His and Glu residues
99 [17], suggesting that an unknown ligand or binding partner exists. Another hookworm-derived
100 ASP-like protein - Neutrophil Inhibitory Factor - has been shown to directly interact with host
101 CD11b, thereby inhibiting neutrophil function [18], hence it remains likely that *Na*-ASP-2 binds to
102 a cell surface receptor from its human host to exert its effector function(s).

103

104 Herein we describe the first probing of a human proteome microarray with a pathogen-derived
105 protein to reveal a selective interaction between *Na*-ASP-2 and CD79A, a component of the B-cell
106 antigen receptor complex. We confirm the interaction by showing that *Na*-ASP-2 binds to human B
107 cells *ex vivo* and triggers changes in B cell-intrinsic gene expression, notably key signaling
108 molecules of the antigen receptor pathway.

109

110 **METHODS**

111

112 **Ethics**

113 Healthy Caucasian volunteers (aged 30-45) from Cairns, Australia, a region that is not endemic for
114 human hookworm infection, were used as a source of peripheral blood under informed consent
115 using a protocol (H4385) approved by the James Cook University Human Research Ethics
116 Committee.

117

118 **Probing of a human protein microarray with recombinant *Na*-ASP-2**

119 Purified, full-length recombinant *Na*-ASP-2 was a kind gift from Dr. Bin Zhan (Baylor College of
120 Medicine, USA). The protein was expressed in *Pichia pastoris* and purified via two ion exchange
121 chromatography steps followed by a final desalting step as described elsewhere [19]. *Na*-ASP-2
122 was biotinylated with NHS-LC-biotin (Thermo-Fisher) and used to probe a Human V5 ProtoArray
123 (Invitrogen) at a final concentration of 50 $\mu\text{g}\cdot\text{ml}^{-1}$. The ProtoArray contains over 9,000 human
124 proteins printed in duplicate, and includes more than 2,600 membrane proteins. Binding of
125 biotinylated *Na*-ASP-2 to proteins on the array was detected with streptavidin Alexafluor 647 at a
126 1:1000 dilution in Protoarray blocking buffer (Invitrogen). The array was scanned using a
127 GeneArray 4000B scanner (Molecular Devices) at 635 nm. Results were saved as a multi-TIFF file
128 and analyzed using Genepix Prospector software, version 7.

129

130 **Molecular Modelling**

131 Comparative modelling was applied to generate a three-dimensional atomic model of human
132 CD79A, using the crystal structure of human CD79B (PDB accession code 3kg5) as a template. A
133 secondary structure-based amino acid sequence alignment of CD79A and CD79B was prepared
134 with SBAL [20] and used to guide the comparative modelling calculations. Twenty independent
135 models were calculated with MODELLER [21], and the one with the lowest energy was selected
136 and superimposed onto one of the monomers in the CD79B homodimer structure (rigid body
137 modelling). The secondary structure topology and amino acid sequence of CD79A is compatible
138 with the intermolecular interactions observed in the CD79 homodimer structure [22]. A minor
139 manual adjustment was made to enable inter-molecular disulphide bond formation (CysA119-
140 CysB136) in the resulting heterodimer. Both cysteine residues were in prime position for this bond,
141 which is also observed in the CD79B homodimer. The crystal structure of *Na*-ASP-2 was docked to
142 the CD79 heterodimer model, using a rigid body approach based on a multi-dimensional spherical
143 polar Fourier correlation with shape and electrostatics expansion as implemented in Hex [23]. The
144 rigid body docking calculations were carried out without preferred contacts to enable an unbiased

145 complex formation. From the generated 100 independent models the highest scoring one (energy
146 score: -873, next highest -720) was chosen. The figures were generated with PyMOL [24].

147

148 **Blood lymphocyte isolation and culture**

149 Human peripheral blood mononuclear cells (PBMCs) were isolated by density centrifugation
150 (LymphoprepTM). Cells (1×10^6 cells.ml⁻¹) were incubated for 4 or 24 h at 37°C in either 96-well
151 plates (for flow cytometry) or 24-well plates (for sort purification) with *Na*-ASP-2 in DMEM with
152 10% heat-inactivated fetal bovine serum, 2 mM L-glutamine, 100 U/mL penicillin, 100 U/mL
153 streptomycin and 25mM HEPES (media). B-cell activation was induced by 24 h of stimulation with
154 10 µg/ml of goat F(ab')₂ anti-human IgM (µ chain, Sigma).

155

156 **Flow cytometry and cell sorting**

157 Cells were stained with fluorophore-conjugated antibodies against CD19 (HIB19), CD20 (2H7),
158 CD3 (OKT3), CD4 (OKT4), CD14 (61D3) CD69 (FN50), HLA-DR (LN3), CD80 (2D10.4), CD86
159 (IT2.2) (all from eBioscience). In experiments using biotinylated *Na*-ASP-2, streptavidin-FITC was
160 included in the staining panel. Cells were analysed using a BD-FACSCantoII flow cytometer.
161 Alternatively, or CD3⁻ CD14⁻ CD19⁺ CD20⁺ cells were sort-purified using a BD-FACSAria III cell
162 sorter.

163

164 **RNA isolation**

165 RNA was extracted from sort-purified CD19⁺ CD20⁺ B cells for high-throughput RNA-Seq at BGI
166 (Hong Kong) or real-time quantitative PCR (qPCR) analysis. Pelleted cells were lysed in RLT
167 buffer (QIAGEN) + beta-mercaptoethanol and stored at -80°C until RNA was extracted using the
168 RNAeasy kit with DNase purification (QIAGEN). The concentration and integrity of each RNA
169 preparation were verified on a 2100 Bioanalyzer (Agilent) and each preparation was stored in
170 RNastable tubes (Biomatrica) at room temperature until subsequent use.

171

172 **Illumina sequencing**

173 RNA was reverse-transcribed to cDNA using the Illumina TruSeq™ sample preparation kit.
174 Briefly, 1.0 µg of total RNA from each cell preparation was used for poly-A mRNA selection using
175 streptavidin-coated magnetic beads. Two rounds of poly-A mRNA enrichment were performed,
176 followed by thermal fragmentation of the mRNA to a length of 100-500 bp. Each fragmented RNA
177 sample was then reverse transcribed to cDNA using random primers, end-repaired and adaptor-
178 ligated (Illumina). Ligated products were PCR-amplified (15 cycles) and cleaned using a MinElute
179 column (QIAGEN). Amplicons were paired-end sequenced on an Illumina HiSeq 2500 (Illumina).

180

181 **Bioinformatic analyses**

182 Ninety bp single-reads were screened for the presence of adapter sequences and sequences with
183 >10% unknown bases and sequences with >50% low-quality bases. The remaining reads were
184 splice-aligned to the human genome reference assembly GRCh37 (NCBI build 37.1) using TopHat,
185 which incorporates the Bowtie v0.11.3 algorithm [25]; subsequently, individual aligned read files
186 were assembled into transcripts using Cufflinks [26]. Relative levels of transcription were measured
187 using the Reads Per Kilobase per Million reads algorithm (RPKM) [27]. Differences in levels of
188 gene transcription were determined as previously described [28]. The false discovery rate method
189 (FDR) [29] was used to correct the errors associated with multiple pairwise comparisons ($FDR \leq$
190 0.001) and a $|\log_2 \text{ratio}| \geq 1$ was set as the threshold for the significance of gene expression changes.
191 Differentially expressed genes (DEGs) were mapped to Gene Ontology terms and Kyoto
192 Encyclopedia of Genes and Genomes (KEGG) biological pathways available in the GO and KEGG
193 databases, respectively (www.geneontology.org; www.genome.jp/kegg/). A hypergeometric test
194 was subsequently used to identify significantly enriched GO terms and KEGG pathways in DEGs
195 compared to the transcriptome background using the GOTerm::Finder software [30]. The calculated
196 *P*-values were subjected to Bonferroni correction using the corrected *P*-value of 0.05 as a threshold.

197 Raw sequence data have been deposited in the Sequence Read Archive (SRA) of NCBI under
198 accession number SRAXXXXXXX.

199

200 **Real-Time quantitative PCR**

201 Total RNA was extracted from sort-purified B cells from four hookworm-naïve Caucasian human
202 volunteers that were cultured for 24 h in the presence or absence of *Na*-ASP-2. cDNAs were
203 prepared using Superscript III reverse transcriptase (Invitrogen). SYBR Green mastermix
204 (QIAGEN) was used with a Rotor-Gene q thermal cycler (QIAGEN). The oligonucleotides were
205 designed manually and synthesized (Integrated DNA Technologies). Data were analyzed using the
206 $\Delta\Delta$ CT method whereby actin served as the endogenous gene and samples were normalized to media
207 controls. Primer sequences were as follows: *β -actin*- forward ATTGGCAATGAGCGGTTC and
208 reverse GGATGCCACAGGACTCCAT; *lyn* forward GAGACTCGGGGAGCCATTG and reverse
209 ACGCTGGGGATGTTATACTCT; *pi3kr5* (23533) forward CTCCACGCTACGTGTTGTG and
210 reverse TGAAGTTTGAAGAACCGTGTGAG.

211

212 **Statistical Analyses**

213 Statistical analyses of qPCR data were conducted using a paired *t* test where $\Delta\Delta$ CT values for each
214 gene of interest were compared between test (*Na*-ASP-2 exposed) vs control (media exposed) cells.
215 *P* values of <0.05 were deemed statistically significant.

216

217 **RESULTS**

218

219 **Interaction between *Na*-ASP-2 and human CD79A revealed by probing of a human proteome 220 microarray**

221 Probing of the human proteome array with biotinylated *Na*-ASP-2 revealed interactions between
222 *Na*-ASP-2 and five human proteins. The strongest interaction was with propionyl-CoA carboxylase

223 (PCCA), an anticipated interaction because PCCA is a biotin-binding enzyme and would therefore
224 be expected to bind to any biotinylated recombinant protein used to probe the array (**Figure 1,**
225 **Supplementary Table 1**). Indeed, we have noted consistent binding of other (unrelated)
226 biotinylated recombinant proteins to PCCA (unpublished). The second most intense association was
227 with CD79A, which together with CD79B forms a hetero-dimer and a subunit of the B-cell antigen
228 receptor. The third and fifth strongest hits were also proteins involved in biotin metabolism
229 (**Supplementary Table 1**). The fourth strongest association was with cortactin, which is involved
230 in actin remodeling and was of sufficiently low signal intensity (2.4 fold lower than CD79A) that
231 we deemed it unworthy of further pursuit (**Supplementary Table 1**). Probing of a second array
232 using identical conditions resulted in consistent binding between *Na*-ASP-2 and the same five
233 human proteins on the array.

234

235 **Modelling of *Na*-ASP-2 interactions with CD79**

236 We recently panned a random 12-mer peptide phage display library with *Na*-ASP-2 and showed
237 that most of the bound peptides were enriched for glutamine and histidine residues [31].
238 Interestingly, the extracellular domain of CD79A contains a HXQXXH motif at residues 51-56.
239 This peptide forms part of a large surface of CD79A which has previously been implicated in
240 binding of the B cell antigen receptor [22]. Rigid body docking of the crystal structure of *Na*-ASP-2
241 and a model of heterodimeric CD79A/CD79B suggests that, based on shape and electrostatics, *Na*-
242 ASP-2 may bind to the CD79 heterodimer (**Figure 2**). Furthermore, this model indicates that *Na*-
243 ASP-2 mainly interacts with the CD79A surface harboring the HXQXXH motif, but a protruding
244 loop of CD79B (residues 79-86) may also engage in interactions with the hookworm protein.

245

246 ***Na*-ASP-2 binds selectively to human B cells.**

247 CD79A is expressed exclusively on B lymphocytes. To verify the interaction between *Na*-ASP-2
248 and CD79A, we cultured human PBMCs from healthy, hookworm-naïve human volunteers ex vivo

249 for 4 or 24 h with biotinylated *Na*-ASP-2 and performed flow cytometry. Cells were stained for B
250 cell markers (CD19, CD20), T cell marker CD3, monocyte marker CD14, and streptavidin-FITC for
251 detection of surface-bound *Na*-ASP-2. This experiment was performed twice, with two different
252 blood donors. As expected, we detected negligible frequencies of FITC⁺ cells following treatment
253 with media or non-biotinylated *Na*-ASP-2, however treatment with increasing amounts of
254 biotinylated *Na*-ASP-2 resulted in a dose-dependent increase in the frequency of *Na*-ASP-2/FITC⁺
255 cells (**Figure 3A**). Gated FITC⁺ cells were analyzed for various leukocyte surface markers. While
256 only 8% of FITC⁺ cells expressed CD3 or CD14, the majority (72%) of FITC⁺ cells co-expressed
257 CD20 and CD19, a phenotype consistent with human B lymphocytes (**Figure 3B**). Modifying
258 culture time, temperature and cell permeabilization state did not enhance the detection of FITC⁺
259 cells (data not shown), but in each case, B cells represented the dominant *Na*-ASP-2/FITC⁺
260 population.

261

262 ***Na*-ASP-2 induces substantial changes in B cell gene expression.**

263 To examine the biological effect of *Na*-ASP-2 on human B cells, we compared the expression of
264 cell activation markers following polyclonal stimulation of the B cell receptor (BCR). PBMCs were
265 treated for 4 h with 2 µg/mL *Na*-ASP-2, or bovine serum albumin (BSA) control and stimulated for
266 24 h with either media, or anti-human IgM. While we did not observe appreciable differences in the
267 expression levels of CD69, CD86, HLA-DR and CD80 on B cells exposed to *Na*-ASP-2 following
268 anti-IgM treatment, we did observe slight but consistent reductions in expression of these markers
269 when cells underwent no exogenous stimulation (**Supplementary Figure 1**). These data suggest
270 that B cells can still be activated in the presence of *Na*-ASP-2, but in the absence of polyclonal
271 stimulation *Na*-ASP-2 may limit the activation state of human B cells.

272

273 In order to investigate the cascade of molecular events that follow binding of *Na*-ASP-2 to human B
274 cells, we sort-purified CD19⁺ CD20⁺ B cells from one volunteer's whole PBMC culture that was

275 treated with either *Na*-ASP-2 or media control and performed RNA-Seq and bioinformatics
276 analyses. B cells that were cultured with *Na*-ASP-2 for 4 h underwent minimal changes in gene
277 expression (37 up-regulated genes, 178 down-regulated genes compared to media control, **Figure**
278 **4A**). After 24 h of culture, however, there was a pronounced bias toward down-regulation of gene
279 expression in B cells that were cultured with *Na*-ASP-2, with 1080 significantly down-regulated
280 genes and only 95 up-regulated genes (**Figure 4B**).

281

282 ***Na*-ASP-2 down-regulates expression of genes involved in multiple biological pathways.**

283 Genes whose expression was significantly altered following exposure to *Na*-ASP-2 were clustered
284 according to their KEGG annotation (**Figure 5**). In particular, the majority of down-regulated genes
285 could be mapped to the ‘cytokine-cytokine receptor interaction’ (ko04060) and the ‘leukocyte
286 transendothelial migration’ (ko04670) pathways, whereas the majority of genes whose expression
287 was up-regulated by *Na*-ASP-2 binding could be mapped to the ‘hematopoietic cell lineage’
288 (ko04640) and ‘chemokine signaling pathway’ (ko04062), respectively.

289

290 ***Na*-ASP-2 down-regulates expression of genes in the Ig receptor (CD79A) signaling pathway.**

291 While *Na*-ASP-2 appears to affect the expression of genes involved in multiple biological
292 pathways, we focused on potential consequences of interactions between *Na*-ASP-2 and CD79A
293 based on our earlier protein-protein interaction studies. In particular, three genes mapping to the
294 KEGG B-cell receptor signaling pathway, i.e. *lyn*, spleen tyrosine kinase (*syk*) and
295 phosphatidylinositol 3-kinase (*pi3k*) displayed significant down-regulation following exposure to
296 *Na*-ASP-2 (**Figure 6**). Each of these gene products are involved in transmitting signals from the
297 BCR and are crucial for essential B-cell functions such as activation, development, proliferation,
298 inhibition and cell death.

299

300 Follow-up studies involving the analysis of B cell-intrinsic gene expression induced by *Na*-ASP-2
301 from four hookworm-naïve blood donors were performed using qPCR. Consistent with our findings
302 from RNA-seq, the expression levels of both *lyn* and *pi3k* were significantly reduced in B cells that
303 were cultured for 24 h with *Na*-ASP-2 ex vivo relative to control cells (**Figure 7**).

304

305 **DISCUSSION**

306 Advances in genomics and proteomics have served to highlight how little we know about the
307 functional interactions of parasitic helminth proteins with their respective hosts tissues [32].
308 Approaches aimed at developing a “portfolio” for a specific pathogen protein of unknown function
309 have provided information on expression, localization and immunogenicity [33]. None of these
310 approaches, however, specifically addresses biochemical function or ligand/receptor interactions.
311 The ES proteins of helminths from diverse phyla have been characterized using proteomics.
312 However, despite the availability of draft genomes for some of these organisms, >50% of genes
313 encoding secreted proteins remain functionally uncharacterized. This is true for *N. americanus*,
314 where 33% of the genome encodes for putatively secreted proteins, but greater than 30% remain un-
315 annotated [34].

316

317 *N. americanus* modulates the human host’s immune system to facilitate its migration from the skin
318 to the lungs en route to the intestine [35]. Immuno-epidemiological studies from human populations
319 have shown that protective acquired immunity to hookworm does not develop in most individuals
320 [36]. One of the means by which hookworms modulate the host’s immune system is via the
321 production of ES proteins [37-40]. The results from our study are consistent with this theory, where
322 we demonstrate that *Na*-ASP-2 interacts with CD79A on human B lymphocytes, suppressing
323 expression of genes that play key roles in multiple biological pathways, including the BCR
324 signaling pathway. While the precise biological function of *Na*-ASP-2/B cell interactions in vivo
325 remains unclear, our in vitro data implies that *Na*-ASP-2 engages CD79A and results in suppression

326 of molecules that determine the activation state of B cells. Our findings neither support nor
327 contradict those of Bower [15] who showed that *Na*-ASP-2 recruits neutrophils. While neutrophils
328 are essential effector cells in acute infections, they also suppress B and T cell responses by
329 competing for antigen with professional antigen presenting cells [41]. Moreover, neutrophils
330 indirectly regulate dendritic cell and T cell interactions [42]. Therefore, *Na*-ASP-2 might serve to
331 suppress immune responses via two distinct but convergent pathways.

332

333 In the absence of experimental three-dimensional structures of *Na*-ASP-2 in complex with host
334 proteins, we generated a model of the *Na*-ASP-2:CD79A:CD79B hetero-trimer complex. This
335 model is in agreement with two previously reported findings. First, the interaction interface between
336 the hookworm protein and the CD79 hetero-dimer has a His/Gln-containing motif with similar
337 properties to those identified by panning a random peptide library with *Na*-ASP-2 [31]. Second, the
338 vast majority of the interaction interface of *Na*-ASP-2 and CD79 is on the α -subunit, coinciding
339 with the interaction interface of CD79 with membrane immunoglobulin [22]. We recently identified
340 the human SK3 channel as a putative receptor of *Na*-ASP-2 based on the presence of a His/Gln-rich
341 peptide that interacted with *Na*-ASP-2 in vitro [31]. Since this His/Gln peptide sequence is only
342 present in one of the isoforms of the SK3 channel (isoform 1), and the human V5 ProtoArray
343 included isoform 2, no interactions with SK3 were observed in this study.

344

345 The human BCR consists of a 1:1 stoichiometry of membrane-bound immunoglobulin and
346 CD79A/CD79B. The immunoglobulin domain relies on a non-covalent association with the
347 CD79A/CD79B heterodimer complex for triggering a signaling cascade [43]. Upon binding of
348 antigen to membrane bound immunoglobulin, the receptor complex undergoes conformational
349 changes, resulting in recruitment of LYN, phosphorylation of the relevant CD79 tyrosines, PI3K
350 recruitment to CD19 and adaptor proteins, and generation of the potent lipid secondary messenger
351 phosphatidylinositol 3,4,5-trisphosphate (PIP3). How interactions between CD79A and *Na*-ASP-2

352 result in down-regulated expression of *lyn* and *pi3k* is unclear, but it is possible that *Na*-ASP-2 may
353 induce an anergic-like state in B cells by preventing BCR clustering and activation of the cell upon
354 antigen binding. Anergic B cells are characterized by impaired propagation of activating signals
355 that are triggered by CD79 engagement [44], substantially reduced PIP3 production [45] and have a
356 dramatically reduced lifespan. While *Na*-ASP-2 does not limit the capacity for B cells to be
357 activated by polyclonal stimulation, the activation state of “resting” B cells appeared to be lowered.
358 Further studies are required to determine if *Na*-ASP-2 can regulate the B cell-intrinsic responses to
359 more physiologically relevant antigens, particularly ES proteins. Hookworms are known to induce a
360 state of immune hypo-responsiveness in chronic infections [36, 46], and by probing a hookworm
361 protein microarray [34] we found that the most heavily infected individuals generated lower IgG
362 responses than did individuals with low or moderate intensity infections (S. Gaze & A. Loukas,
363 unpublished). These findings serve to highlight the altered B cell functions in individuals with
364 heavy hookworm infection, and offer a potential causative role for proteins such as *Na*-ASP-2,
365 however this hypothesis requires rigorous testing, potentially in well-controlled hookworm dose-
366 ranging studies [47].

367

368 To our knowledge this is the first report of a pathogen protein that interacts with the BCR, or
369 modulates expression of signaling molecules that determine B-cell function. Given the interest in
370 hookworm-secreted proteins for treating autoimmune and allergic diseases [40, 48], our findings
371 suggest that *Na*-ASP-2 warrants testing as a novel biologic for treating B cell-mediated
372 autoimmunity. Administration of anti-CD79 or anti-CD79B monoclonal antibodies prevent
373 collagen-induced arthritis [49] or lupus [50], respectively in mice, offering the potential for reduced
374 side effects whilst maintaining B cells in a transient anergic state that does not require their
375 depletion. Thus, *Na*-ASP-2 could prove beneficial as a treatment for autoimmune B cell-mediated
376 diseases such as Multiple Sclerosis or rheumatoid arthritis.

377

378 Our findings herein highlight the novel application of protein microarray technology to addressing
379 host-hookworm interactions at the protein level, and provide a powerful and rapid screening process
380 that could be applied to the study and identification of interactions between other pathogens and
381 host proteins. By coupling the probing of the human proteome array with ex vivo confirmation of
382 binding to live cells and subsequent NGS to determine changes in gene expression, we have
383 demonstrated the utility of this pipeline for elucidating novel host-pathogen interactions and
384 assigning functions to that enigmatic group of pathogen molecules that are frustratingly referred to
385 as “proteins of unknown function”.

386

387 ***Acknowledgements.***

388 We thank Drs Peter Hotez, Maria Elena Bottazzi, Bin Zhan, Soraya Gaze, Travis Beddoe and Phil
389 Felgner for helpful discussion and provision of reagents.

390

391 **REFERENCES**

- 392 1. Hotez PJ, Bethony JM, Diemert DJ, Pearson M, Loukas A. Developing vaccines to combat
393 hookworm infection and intestinal schistosomiasis. *Nat Rev Microbiol* **2010**; 8:814-26.
- 394 2. Palmer ED. Course of egg output over a 15 year period in a case of experimentally induced
395 necatoriasis americanus, in the absence of hyperinfection. *Am J Trop Med Hyg* **1955**; 4:756-7.
- 396 3. Albonico M, Smith PG, Ercole E, et al. Rate of reinfection with intestinal nematodes after
397 treatment of children with mebendazole or albendazole in a highly endemic area. *Trans R Soc*
398 *Trop Med Hyg* **1995**; 89:538-41.
- 399 4. Loukas A, Bethony J, Brooker S, Hotez P. Hookworm vaccines: past, present, and future. *Lancet*
400 *Infect Dis* **2006**; 6:733-41.
- 401 5. Fujiwara RT, Loukas A, Mendez S, et al. Vaccination with irradiated *Ancylostoma caninum* third
402 stage larvae induces a Th2 protective response in dogs. *Vaccine* **2006**; 24:501-9.
- 403 6. Bethony J, Loukas A, Smout M, et al. Antibodies against a secreted protein from hookworm
404 larvae reduce the intensity of hookworm infection in humans and vaccinated laboratory animals.
405 *FASEB J* **2005**; 19:1743-5.
- 406 7. Bethony JM, Simon G, Diemert DJ, et al. Randomized, placebo-controlled, double-blind trial of
407 the *Na*-ASP-2 hookworm vaccine in unexposed adults. *Vaccine* **2008**; 26:2408-17.
- 408 8. Diemert DJ, Pinto AG, Freire J, et al. Generalized urticaria induced by the *Na*-ASP-2 hookworm
409 vaccine: implications for the development of vaccines against helminths. *J Allerg Clin Immunol*
410 **2012**; 130:169-76 e6.
- 411 9. Zhan B, Santiago H, Keegan B, et al. Fusion of *Na*-ASP-2 with human immunoglobulin
412 Fc γ abrogates histamine release from basophils sensitized with anti-*Na*-ASP-2 IgE.
413 *Parasite Immunol* **2012**; 34:404-11.
- 414 10. Hazebrouck S, Guillon B, Drumare MF, Paty E, Wal JM, Bernard H. Trypsin resistance of the
415 major peanut allergen Ara h 6 and allergenicity of the digestion products are abolished after
416 selective disruption of disulfide bonds. *Mol Nutr Food Res* **2012**; 56:548-57.

- 417 11. Koyanagi S, Murakami T, Maeda T, et al. Production-scale purification of the recombinant
418 major house dust mite allergen Der f 2 mutant C8/119S. *J Biosci Bioeng* **2010**; 110:597-601.
- 419 12. Winkler B, Bolwig C, Seppala U, Spangfort MD, Ebner C, Wiedermann U. Allergen-specific
420 immunosuppression by mucosal treatment with recombinant Ves v 5, a major allergen of
421 *Vespula vulgaris* venom, in a murine model of wasp venom allergy. *Immunology* **2003**;
422 110:376-85.
- 423 13. Bungiro R, Cappello M. Twenty-first century progress toward the global control of human
424 hookworm infection. *Curr Infect Dis Rep* **2011**; 13:210-7.
- 425 14. Hotez PJ, Hawdon JM, Cappello M, et al. Molecular approaches to vaccinating against
426 hookworm disease. *Pediatr Res* **1996**; 40:515-21.
- 427 15. Bower MA, Constant SL, Mendez S. *Necator americanus*: the *Na*-ASP-2 protein secreted by
428 the infective larvae induces neutrophil recruitment in vivo and in vitro. *Exp Parasitol* **2008**;
429 118:569-75.
- 430 16. Osman A, Wang CK, Winter A, et al. Hookworm SCP/TAPS protein structure--A key to
431 understanding host-parasite interactions and developing new interventions. *Biotech Adv* **2012**;
432 30:652-7.
- 433 17. Asojo OA, Goud G, Dhar K, et al. X-ray structure of *Na*-ASP-2, a pathogenesis-related-1
434 protein from the nematode parasite, *Necator americanus*, and a vaccine antigen for human
435 hookworm infection. *J Mol Biol* **2005**; 346:801-14.
- 436 18. Rieu P, Ueda T, Haruta I, Sharma CP, Arnaout MA. The A-domain of beta 2 integrin CR3
437 (CD11b/CD18) is a receptor for the hookworm-derived neutrophil adhesion inhibitor NIF. *J Cell*
438 *Biol* **1994**; 127:2081-91.
- 439 19. Goud GN, Bottazzi ME, Zhan B, et al. Expression of the *Necator americanus* hookworm larval
440 antigen *Na*-ASP-2 in *Pichia pastoris* and purification of the recombinant protein for use in
441 human clinical trials. *Vaccine* **2005**; 23:4754-64.

- 442 20. Wang CK, Broder U, Weeratunga SK, Gasser RB, Loukas A, Hofmann A. SBAL: a practical
443 tool to generate and edit structure-based amino acid sequence alignments. *Bioinformatics* **2012**;
444 28:1026-7.
- 445 21. Sali A, Blundell TL. Comparative protein modelling by satisfaction of spatial restraints. *J Mol*
446 *Biol* **1993**; 234:779-815.
- 447 22. Radaev S, Zou Z, Tolar P, et al. Structural and functional studies of Igalphabeta and its
448 assembly with the B cell antigen receptor. *Structure* **2010**; 18:934-43.
- 449 23. Ritchie DW, Kozakov D, Vajda S. Accelerating and focusing protein-protein docking
450 correlations using multi-dimensional rotational FFT generating functions. *Bioinformatics* **2008**;
451 24:1865-73.
- 452 24. The PyMOL Molecular Graphics System, Version 1.5.0.4 Schrödinger, LLC.
- 453 25. Langmead B, Trapnell C, Pop M, Salzberg SL. Ultrafast and memory-efficient alignment of
454 short DNA sequences to the human genome. *Genome Biol* **2009**; 10:R25.
- 455 26. Trapnell C, Williams BA, Pertea G, et al. Transcript assembly and quantification by RNA-Seq
456 reveals unannotated transcripts and isoform switching during cell differentiation. *Nat Biotechnol*
457 **2010**; 28:511-5.
- 458 27. Mortazavi A, Williams BA, McCue K, Schaeffer L, Wold B. Mapping and quantifying
459 mammalian transcriptomes by RNA-Seq. *Nat Methods* **2008**; 5:621-8.
- 460 28. Audic S, Claverie JM. The significance of digital gene expression profiles. *Genome Res* **1997**;
461 7:986-95.
- 462 29. Benjamini Y, Drai D, Elmer G, Kafkafi N, Golani I. Controlling the false discovery rate in
463 behavior genetics research. *Behav Brain Res* **2001**; 125:279-84.
- 464 30. Boyle EI, Weng S, Gollub J, et al. GO::TermFinder--open source software for accessing Gene
465 Ontology information and finding significantly enriched Gene Ontology terms associated with a
466 list of genes. *Bioinformatics* **2004**; 20:3710-5.

- 467 31. Mason L, Tribolet L, Simon A, et al. Probing the equatorial groove of the hookworm protein
468 and vaccine candidate antigen, *Na*-ASP-2. *Int J Biochem Cell Biol* **2014**; 50:146-55.
- 469 32. Bird DM, Opperman CH. The secret(ion) life of worms. *Genome Biol* **2009**; 10:205.
- 470 33. Doyle S. Fungal proteomics: from identification to function. *FEMS Microbiol Lett* **2011**; 321:1-
471 9.
- 472 34. Tang YT, Gao X, Rosa BA, et al. Genome of the human hookworm *Necator americanus*. *Nat*
473 *Genet* **2014**; 46:261-9.
- 474 35. Bethony J, Brooker S, Albonico M, et al. Soil-transmitted helminth infections: ascariasis,
475 trichuriasis, and hookworm. *Lancet* **2006**; 367:1521-32.
- 476 36. Loukas A, Constant SL, Bethony JM. Immunobiology of hookworm infection. *FEMS Immunol*
477 *Med Microbiol* **2005**; 43:115-24.
- 478 37. McSorley HJ, Loukas A. The immunology of human hookworm infections. *Parasite Immunol*
479 **2010**; 32:549-59.
- 480 38. Gaze S, McSorley HJ, Daveson J, et al. Characterising the mucosal and systemic immune
481 responses to experimental human hookworm infection. *PLoS Path* **2012**; 8:e1002520.
- 482 39. Ferreira I, Smyth D, Gaze S, et al. Hookworm excretory/secretory products induce interleukin-4
483 (IL-4)+ IL-10+ CD4+ T cell responses and suppress pathology in a mouse model of colitis.
484 *Infect Immun* **2013**; 81:2104-11.
- 485 40. Navarro S, Ferreira I, Loukas A. The hookworm pharmacopoeia for inflammatory diseases. *Int J*
486 *Parasitol* **2013**; 43:225-31.
- 487 41. Yang CW, Strong BS, Miller MJ, Unanue ER. Neutrophils influence the level of antigen
488 presentation during the immune response to protein antigens in adjuvants. *J Immunol* **2010**;
489 185:2927-34.
- 490 42. Yang X, Gao X. Role of dendritic cells: a step forward for the hygiene hypothesis. *Cell Mol*
491 *Immunol* **2011**; 8:12-8.
- 492 43. Treanor B. B-cell receptor: from resting state to activate. *Immunology* **2012**; 136:21-7.

- 493 44. O'Neill SK, Getahun A, Gauld SB, et al. Monophosphorylation of CD79a and CD79b ITAM
494 motifs initiates a SHIP-1 phosphatase-mediated inhibitory signaling cascade required for B cell
495 anergy. *Immunity* **2011**; 35:746-56.
- 496 45. Browne CD, Del Nagro CJ, Cato MH, Dengler HS, Rickert RC. Suppression of
497 phosphatidylinositol 3,4,5-trisphosphate production is a key determinant of B cell anergy.
498 *Immunity* **2009**; 31:749-60.
- 499 46. Fujiwara RT, Cancado GG, Freitas PA, et al. *Necator americanus* infection: a possible cause of
500 altered dendritic cell differentiation and eosinophil profile in chronically infected individuals.
501 *PLoS Negl Trop Dis* **2009**; 3:e399.
- 502 47. Fujiwara RT, Cancado GG, Freitas PA, et al. *Necator americanus* infection: a possible cause of
503 altered dendritic cell differentiation and eosinophil profile in chronically infected individuals.
504 *PLoS Negl Trop Dis* **2009**; 3:e399.
- 505 48. Mortimer K; Brown A, Feary J, et al. Dose-ranging study for therapeutic infection with *Necator*
506 *americanus* in humans. *Am J Trop Med Hyg* **2006**; 75: 914-20.
- 507 49. Hardy IR, Anceriz N, Rousseau F, et al. Anti-CD79 Antibody Induces B Cell Anergy That
508 Protects against Autoimmunity. *J Immunol* **2014**; 192:1641-50.
- 509 50. Li Y, Chen F, Putt M, et al. B cell depletion with anti-CD79 mAbs ameliorates autoimmune
510 disease in MRL/lpr mice. *J Immunol* **2008**; 181:2961-72.

511

512

513 **FIGURE LEGENDS**

514 **Figure 1. Binding of biotinylated *Na*-ASP-2 to CD79A and biotin-binding proteins on a**
515 **Human V5 ProtoArray.** The array was probed with biotinylated recombinant *Na*-ASP-2 followed
516 by streptavidin Alexafluor 647 and scanned using a GeneArray 4000B scanner at 635 nm using
517 laser intensity settings of 100% (A) and 66% (B). Yellow boxes denote the area of the array
518 containing duplicate spots of CD79A and PCCA. Panel C shows a magnified view of the area
519 contained within the yellow boxes. All other spots are positive control proteins spotted in duplicate
520 to allow orientation on the array. Two separate arrays were probed independently, with
521 representative results from one experiment displayed.

522

523 **Figure 2. Rigid body models of the CD79A/CD79B heterodimer (A) and the**
524 **CD79A/CD79B:*Na*-ASP-2 complex (B).** CD79A is coloured wheat, CD79B pale green, and *Na*-
525 ASP-2 is coloured magenta. Cysteine residues and disulphide bonds are rendered as sticks in
526 yellow. The CD79A peptide HFQCPH (residues 51-56) is coloured blue. Surface representation of
527 the CD79 heterodimer model (A). Cartoon rendering of the modelled ternary complex of *Na*-ASP-2
528 and CD79 (B).

529

530 **Figure 3. *Na*-ASP-2 binds selectively to human B-cells.** PBMCs from hookworm-naïve donor
531 volunteers were cultured for 24 h in the presence of increasing concentrations of biotinylated
532 recombinant *Na*-ASP-2, or with unlabeled *Na*-ASP-2. (A) Frequencies of cells with biotinylated
533 *Na*-ASP-2 on the surface were quantified by flow cytometry after incubation with FITC-conjugated
534 streptavidin. (B) *Na*-ASP-2⁺ FITC⁺ cells were gated for analysis of the immune cell-surface
535 markers CD3, CD14, CD20 and CD19. Experiments were conducted twice, with two different
536 blood donors; representative data are shown.

537

538 **Figure 4. Changes in mRNA expression in B cells from a hookworm-naïve human volunteer**
539 **after culture with *Na*-ASP-2.** PBMCs were cultured for 4 or 24 h with either media or 2 $\mu\text{g}\cdot\text{ml}^{-1}$
540 *Na*-ASP-2; CD19⁺ CD20⁺ B cells were sort purified and isolated RNA was subjected to RNA Seq
541 analysis. Scatter plots comparing log₂ ratios of RPKM expression values for B cells from a
542 hookworm-naïve human volunteer following ex vivo co-culture with *Na*-ASP-2 at 4 and 24 hours.
543 Numbers indicate the numbers of up or down-regulated genes.

544

545 **Figure 5. Differential gene expression following 24 h exposure to *Na*-ASP-2.** Heatmap analysis
546 of differentially expressed genes following 24 h culture of sort-purified human B cells with *Na*-
547 ASP-2. Differentially expressed genes are clustered according to their KEGG annotation. The top
548 KEGG pathways assigned to the majority of genes within each cluster are also reported.

549

550 **Figure 6. *Na*-ASP2 causes B-cell intrinsic reductions in expression of mRNAs immediately**
551 **downstream of CD79A.** Schematic representation of the B cell receptor signaling pathway
552 (modified from http://www.genome.jp/kegg-bin/show_pathway?hsa04662). Genes whose
553 expression was down-regulated following 24 h -co-culture of B cells with *Na*-ASP-2 are indicated
554 by green boxes.

555

556 **Figure 7. Down-regulated expression of *lyn* and *pi3k* in human B cells from four hookworm-**
557 **naïve human volunteers after culture with *Na*-ASP-2.** PBMCs from four hookworm-naïve donor
558 volunteers were cultured for 24 h in the presence of medium alone or 2 $\mu\text{g}\cdot\text{ml}^{-1}$ recombinant *Na*-
559 ASP-2. qPCR analysis of *lyn* and *pi3kR5* was performed on RNA derived from sort-purified B cells.
560 Data were analyzed using the $\Delta\Delta\text{CT}$ method (Relative quantification, RQ), whereby actin served as
561 the endogenous gene and samples were normalized to media controls. *P = 0.0295; **P = 0.0004.

562 **Supplementary Figure 1: Impact of *Na*-ASP-2 on B cell expression of activation surface**
563 **markers following anti-IgM-stimulation and in the steady-state.** PBMCs from hookworm-naïve
564 volunteers were pre-incubated for 4 h with 2 µg/mL of either a control protein (BSA) or *Na*-ASP-2
565 prior to incubation for 24 h with 10 µg/ml goat F(ab')₂ anti-mouse IgM or media alone (No
566 treatment). Surface marker expression on gated CD19⁺ CD20⁺ B cells was compared by flow
567 cytometry. Color-coded numbers in each inset represents mean fluorescence intensity for each
568 marker. The experiment was performed twice, with a different blood donor each time;
569 representative data are shown.

Figure 1
[Click here to download high resolution image](#)

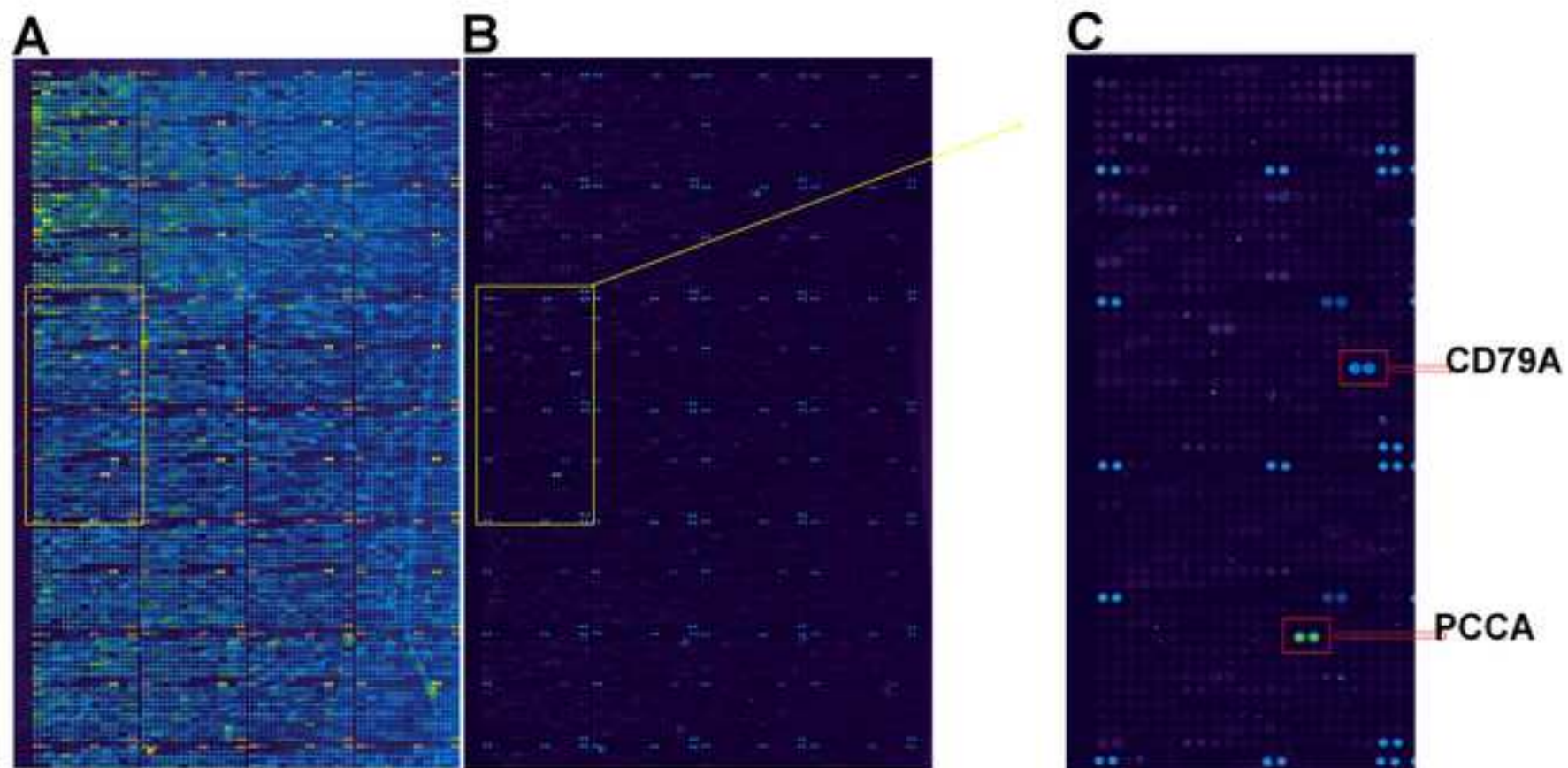


Figure 2
[Click here to download high resolution image](#)

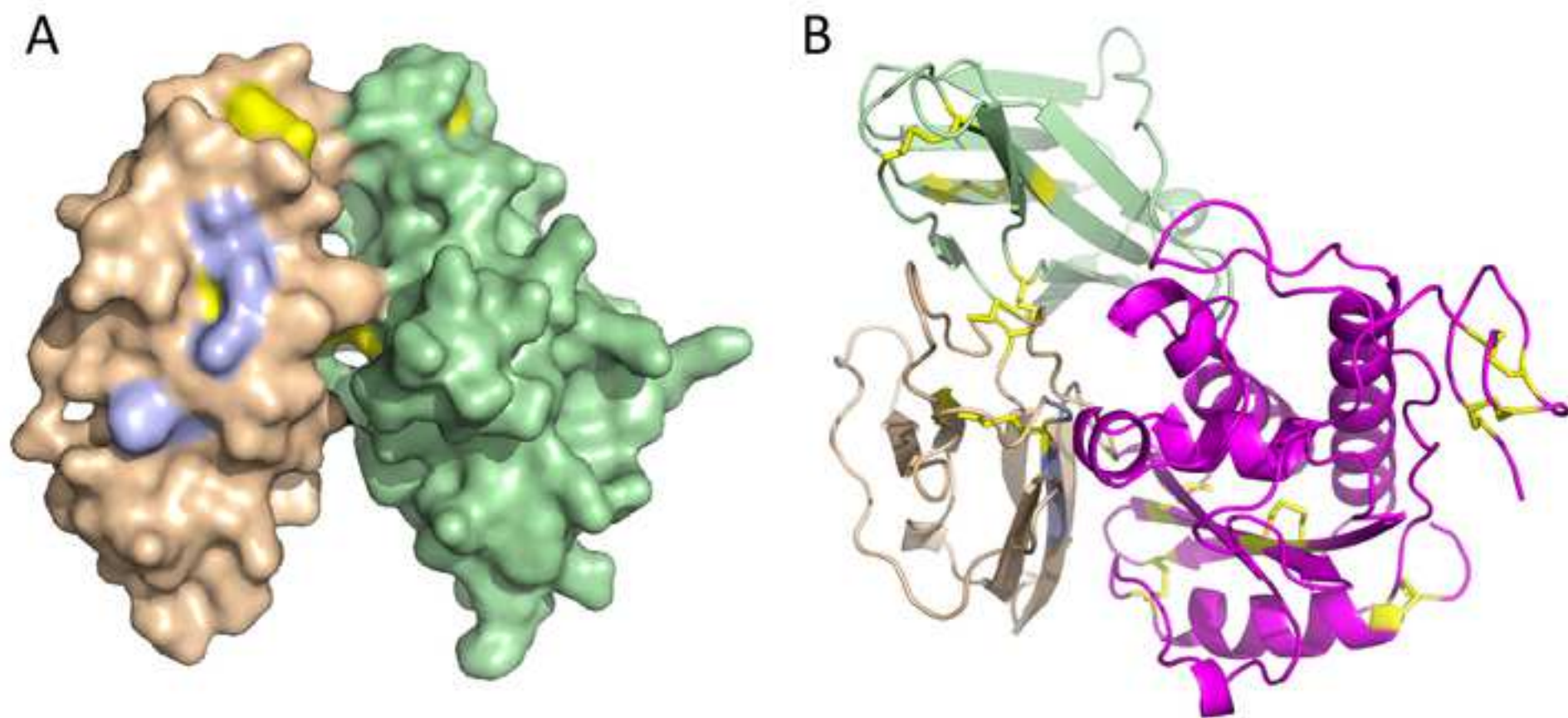


Figure 3
[Click here to download high resolution image](#)

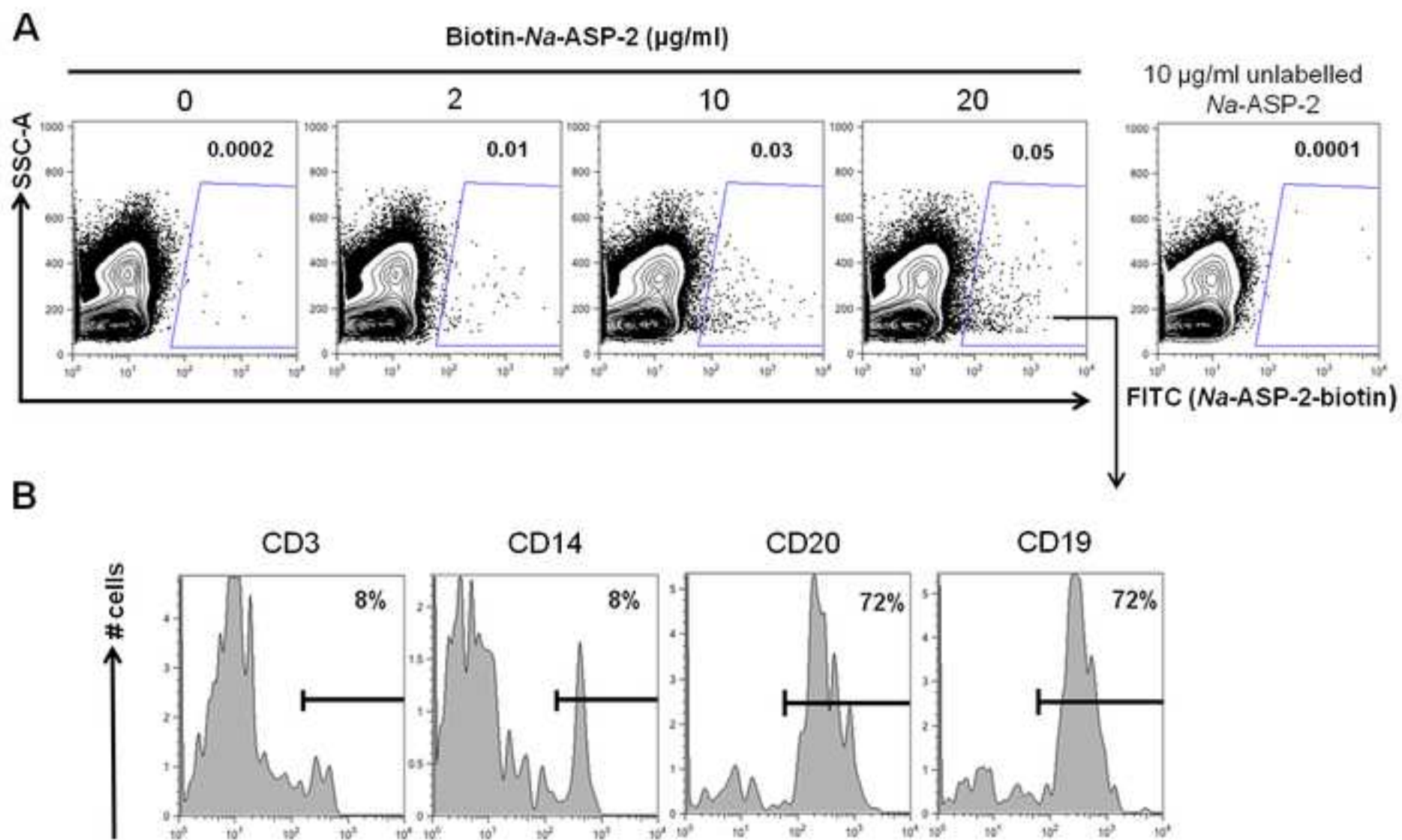


Figure 4
[Click here to download high resolution image](#)

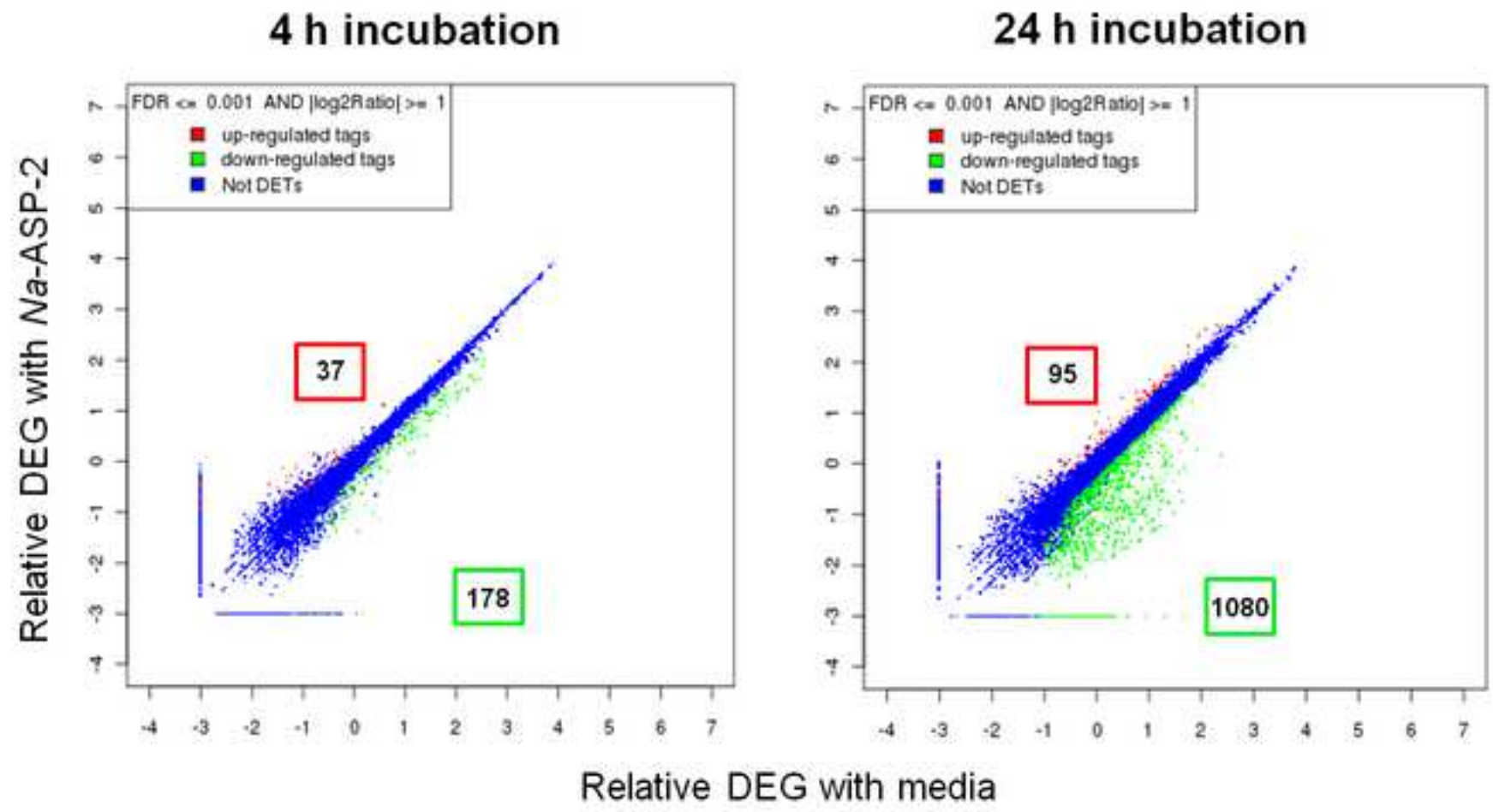


Figure 5
[Click here to download high resolution image](#)

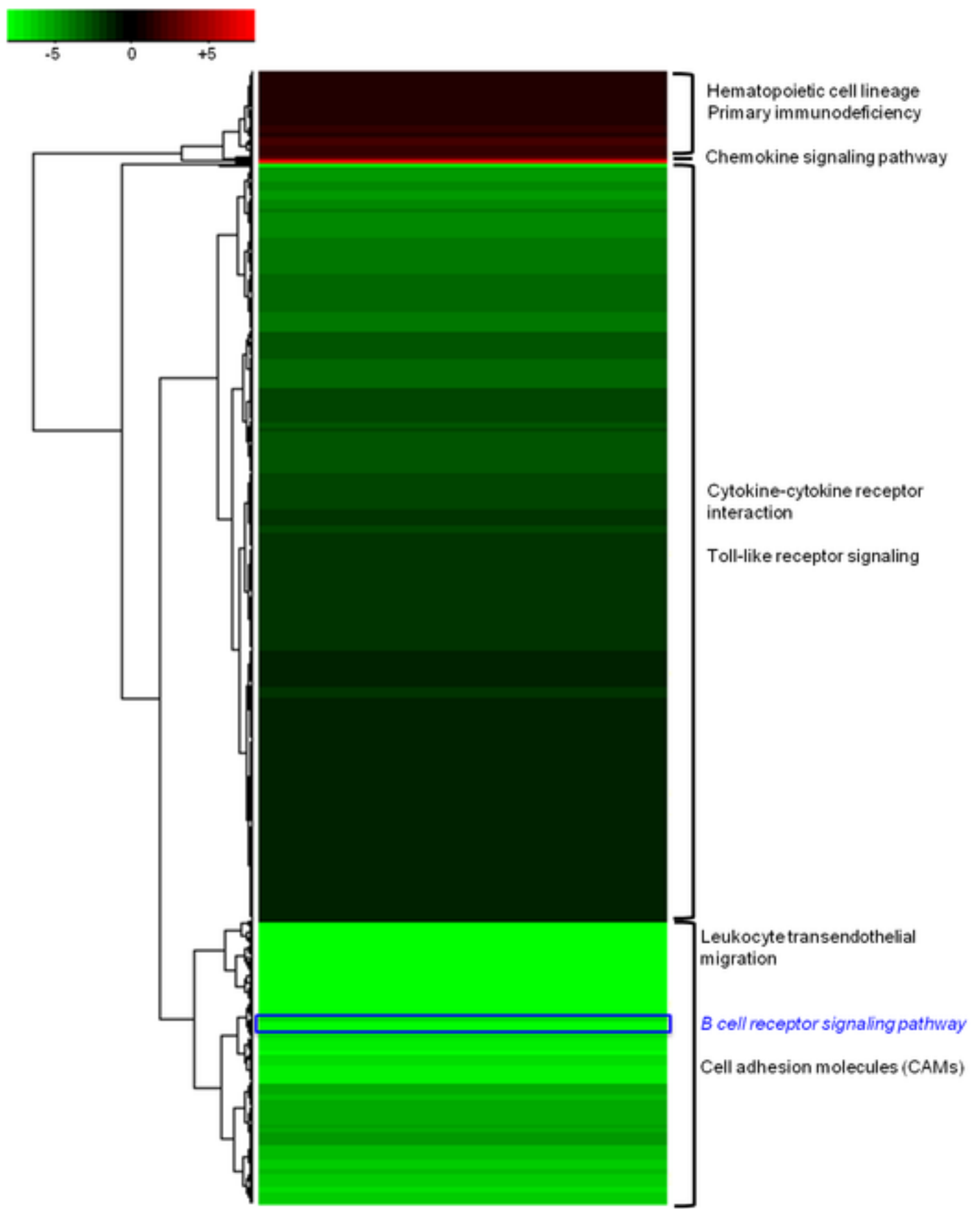


Figure 6
[Click here to download high resolution image](#)

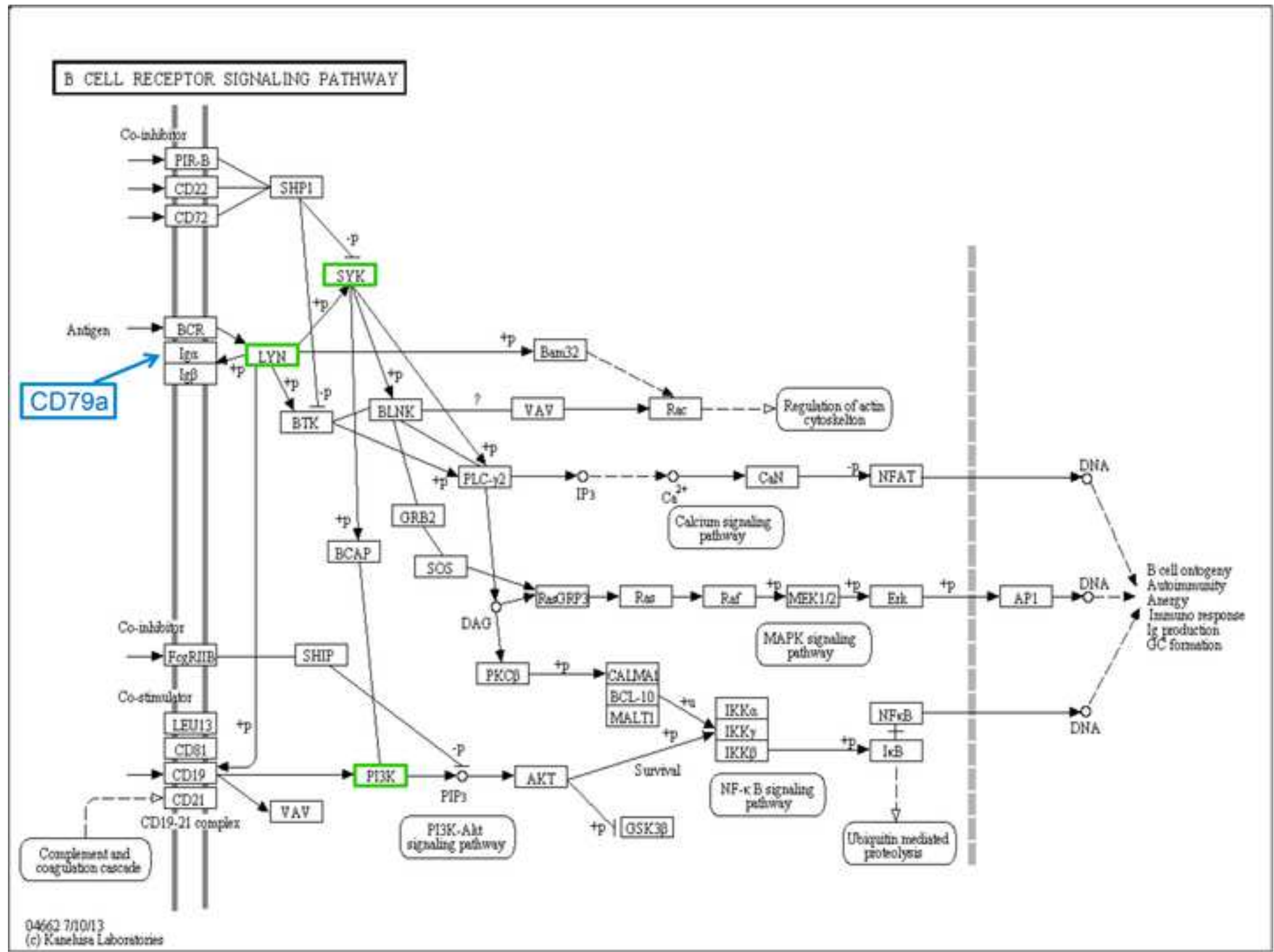
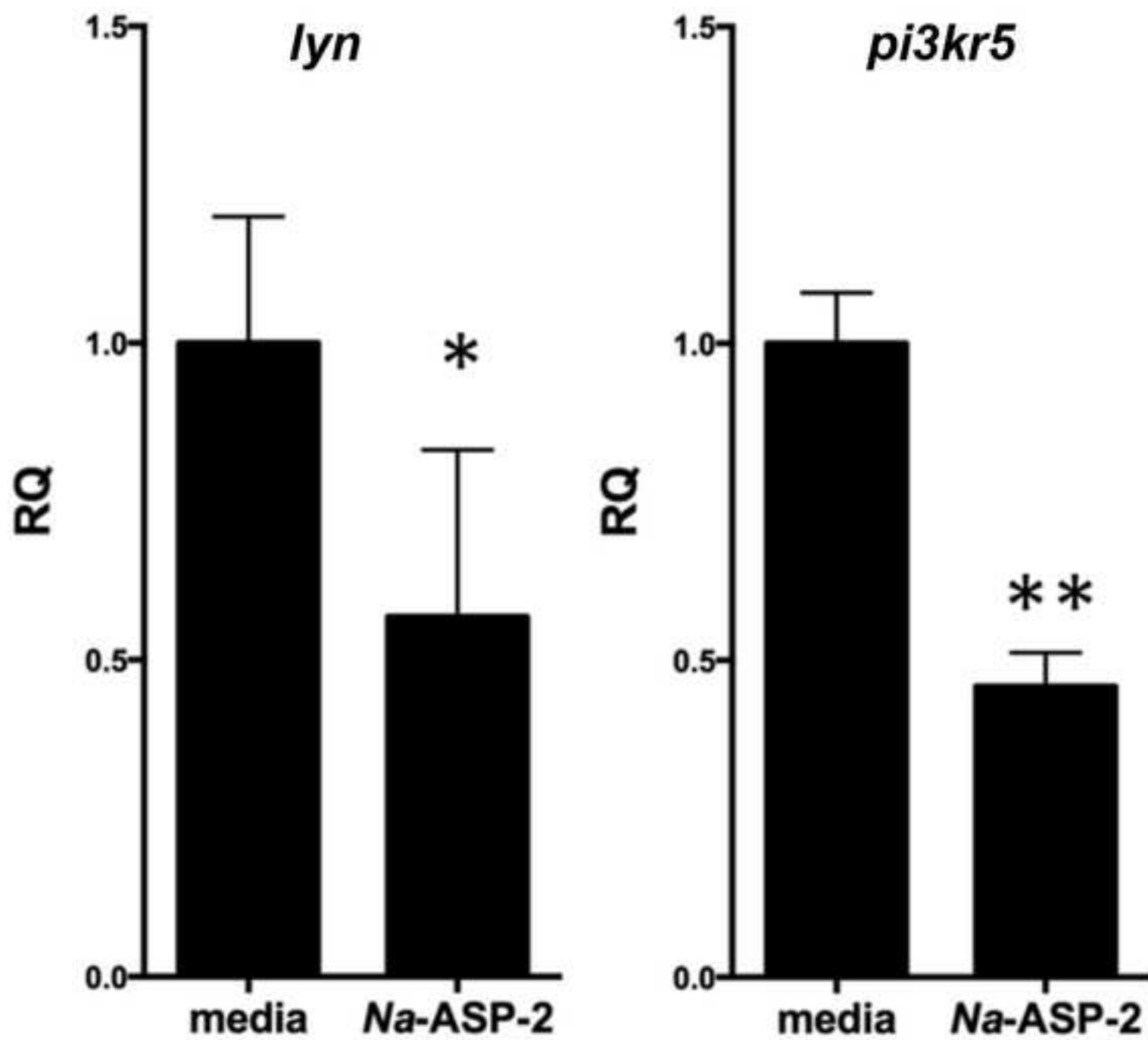


Figure 7
[Click here to download high resolution image](#)



Supplementary Table 1- List of proteins on the Human V5 ProtoArray that interacted with recombinant *Na*-ASP-2.

Intensity	Protein	NCBI code	Description
1600	Propionyl coenzyme A carboxylase (PCCA)	NM_000282.1	Biotin binding enzyme
456.5	Immunoglobulin binding protein 1 (IGBP1/CD79a)	NM_001551.1	Co-receptor of B-cell receptor complex
359.5	Methylcrotonoyl-Coenzyme A carboxylase 1 (alpha) (MCCC1)	NM_020166.2	Biotin metabolism
191.5	Cortactin (CTTN), transcript variant 2, intracellular	NM_138565.1	Actin remodelling enzyme
177.5	Enoyl-Coenzyme A, hydratase/3-hydroxyacyl Coenzyme A dehydrogenase (EHHADH)	BC000306.1	Biotin metabolism

